The relationship between fatigue strength and microstructure in an austempered Cu–Ni–Mn–Mo alloyed ductile iron

M. BAHMANI, R. ELLIOTT
Manchester Materials Science Centre, University of Manchester, Grosvenor Street, Manchester, M1 7HS, UK

N. VARAHRAM
Sharif University of Technology, Tehran, Iran

Rotating bending fatigue measurements are reported for an austempered ductile iron containing 3.5 wt % C, 2.6 wt % Si, 0.48 wt % Cu, 0.96 wt % Ni, 0.27 wt % Mo, and 0.25 wt % Mn. The iron was austenitized at 870, 900 and 950 °C and then austempered at 370 and 400 °C for times between 30 and 240 min to obtain various austempered microstructures. The correlation between fatigue strength and austempered microstructure represented by the parameter $X_\gamma C_\gamma$, where X_γ is the amount of high C austenite and C_γ its C content is examined. It is shown that fatigue strength increases as $X_\gamma C_\gamma$ increases. The highest fatigue strength is obtained with an ausferrite structure; the presence of martensite and/or carbide in the structure reduces the fatigue strength. Lower austenitizing temperatures increase the fatigue strength.

1. Introduction

Austempered ductile iron, ADI, is now a well established member of the cast iron family. It offers high strength, toughness, ductility and wear resistance properties. Early applications such as gears and agricultural components used the high wear resistance coupled with strength and good toughness. The continued expansion of ADI will depend on applications for high ductility grades, for example, crankshafts [1–3]. Fatigue properties are important in such applications and although several studies have been reported the relationship between fatigue strength and austempered microstructure has not been established fully.

Several studies [4–8] have shown that austempering increases the fatigue strength of ductile iron. However, limitations to the increment in fatigue strength have been associated with variations in processing, improper feeding of castings, nodule size, nodularity and inclusions. Studies by Faubert *et al.* [9–10] on a completely ausferrite (ferrite plus high C austenite) austempered structure in a heavy section alloyed ADI confirm that the rotating bending fatigue strength is 45–60% higher than in a pearlitic as-cast structure. In addition, the fatigue strength in both the austempered and as-cast conditions showed only a small sensitivity to position within the casting. The difference in fatigue strength in the best and worst conditions was only 15%. This led to the suggestion that fatigue strength is dependent primarily on the structure of the austempered matrix and residual stress. Similar conclusions were drawn from parallel studies [11] on unalloyed irons. The fatigue strength, in contrast to tensile properties, of the unalloyed iron was only marginally better than that of the alloyed iron. More recently, studies by Shanmugam *et al.* [12] have suggested that the rotating bending fatigue shows a well defined relationship to austenitizing temperature and the amount and carbon content of the high C austenite phase as measured by the parameter $X_\gamma C_\gamma$. However, the majority of these measurements were made with an austempering temperature of 280 °C at which high strength grades of ADI are produced. Therefore, the present study concentrates on high ductility grades by using different combinations of austenitizing temperature (870, 900 and 950 °C) and austempering temperatures (370 and 400 °C) to investigate the correlation between austempered microstructure and fatigue strength further.

2. Experimental procedure

The iron used was of composition 3.5 wt % C, 2.6 wt % Si, 0.48 wt % Cu, 0.96 wt % Ni, 0.27 wt % Mo and 0.25 wt % Mn. It was produced in the form of 75 mm keel blocks in a commercial foundry using electric melting. All specimens were taken from the bottom half of the keel block in order to avoid structural defects. Details have been given in the companion paper [3] of specimen dimensions and the X-ray diffraction and quantitative metallographic techniques used to follow the evolution of the

0022–2461

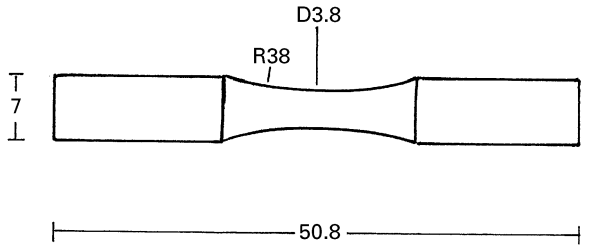

Figure 1 Fatigue specimen dimensions (mm).

austempered microstructure. Details were given also of the austenitizing and austempering heat treatment procedures. For the fatigue studies bars of 80 mm length and 8 mm diameter were machined from the middle of the bottom section of the keel blocks. These bars were austempered before unnotched fatigue specimens, with the dimensions shown in Fig. 1, were machined from the bars. After machining, hand polishing was carried out using successively fine grades of emery paper followed by 1 μm diamond paste until all circumferential markings were removed. Rotating bending fatigue tests were performed at different stress levels using a Bristol Engineering Division testing machine. At least ten specimens were tested for each heat treated condition.

3. Results and discussion

3.1. As-cast properties

The as-cast iron showed a bull's eye structure with ferrite surrounding the graphite nodules in a pearlitic matrix with a few intercellular carbides. Quantitative analysis showed there was 79% pearlite, 9.5% ferrite and 11.5% graphite present in the structure. The nodule count in the bottom section of the keel block was 90–100 mm^{-2} with a nodularity of 78–80%. Fig. 2 shows measurements of the rotating bending fatigue properties in the as-cast and austempered states. These results confirm that the fatigue strength is increased by austempering.

3.2. Fatigue properties of austempered irons

Fig. 3 shows how the ultimate tensile strength (UTS) and fatigue strength measured in the present study varies with austempering temperature for a constant austenitizing temperature of 900 °C and austempering time of 90 min. The figure also shows similar results due to Grech and Young [8] but for an iron of composition 2.3 wt % C, 2.5 wt % Si, 0.21 wt % Mn, 1.6 wt % Cu and 1.6 wt % Ni after austenitizing at 900 °C and austempering for 240 min. Both studies show that the rotating bending fatigue strength does not show a simple relationship with tensile strength. Maximum fatigue strength is associated with treatments that give maximum ductility and high retained austenite levels. Fatigue measurements were made as a function of austempering time at 370 °C for austenitizing temperatures of 870, 900 and 950 °C in order to study the influence of matrix structure on the fatigue strength. These results are shown in Table I with corresponding measurements of retained austenite content, X_γ, unreacted austenite content, X_γ^0, and the parameter $X_\gamma C_\gamma$.

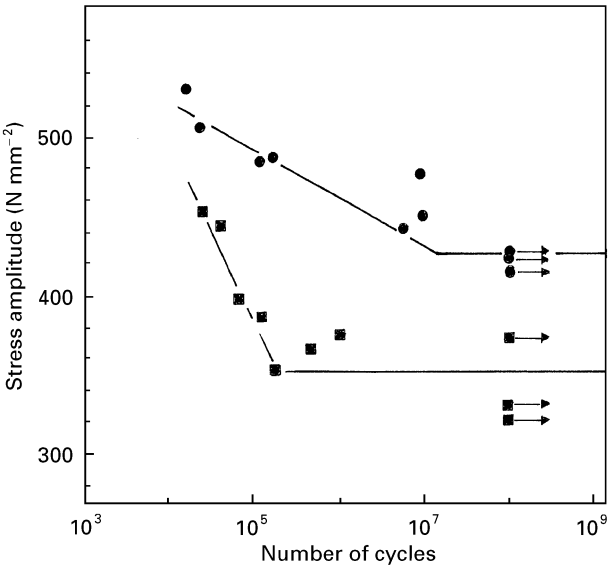

Figure 2 Rotating bending fatigue measurements in the as-cast (■) condition and after austenitizing at 900 °C for 120 min and austempering at 370 °C for 120 min (●). The arrows indicate that the specimens had not fractured after 10^8 cycles. The horizontal fatigue strength line was obtained by selecting the lowest stress fracture at less than 10^8 cycles or the highest stress at which 10^8 cycles were incurred whichever was the lower.

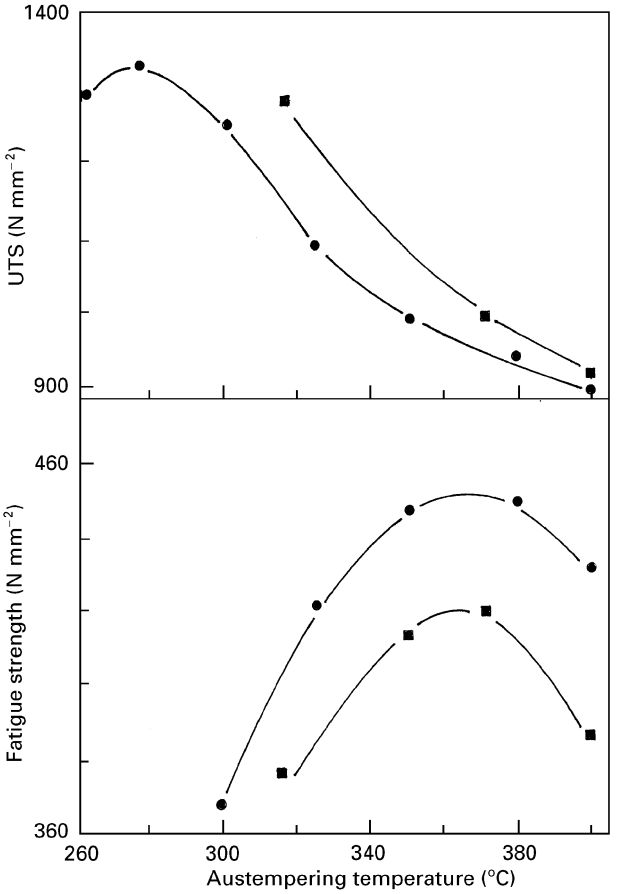

Figure 3 Variation of UTS and fatigue strength with austempering temperature: (■) present study, irons austenitized at 900 °C, austempered for 90 min; and (●) due to Grech and Young [8], irons austenitized at 900 °C, austempered for 240 min.

TABLE I Fatigue strength and austempered microstructure characteristics

Austempering treatment[a]	X_γ (wt %)	$X_\gamma C_\gamma$ (wt %)	X_γ^0 (wt %)	Fatigue strength ($N\,mm^{-2}$)
As-cast	0.00	0.00	0.00	345
At 870 °C/370 °C for 30 min	0.28	0.60	0.035	406
90 min	0.27	0.64	0.020	418
120 min	0.25	0.55	0.008	415
240 min	0.22	0.44	0.006	383
At 900 °C/370 °C for 30 min	0.38	0.68	0.090	397
90 min	0.40	0.72	0.040	420
120 min	0.38	0.68	0.035	421
240 min	0.34	0.56	0.030	400
At 950 °C/370 °C for 30 min	0.42	0.82	0.150	362
90 min	0.43	0.83	0.090	380
120 min	0.45	0.81	0.070	387
240 min	0.44	0.76	0.060	384
At 870 °C/400 °C for 90 min	0.35	0.58	0.025	392
At 900 °C/400 °C for 90 min	0.38	0.65	0.090	385
At 900 °C/350 °C for 90 min	–	–	–	415
At 900 °C/315 °C for 90 min	0.20	0.38	–	376

[a] Measurements made as a function of austempering time at 370 °C (with the exception of the last four heading) for austenitizing temperatures of 870, 900 and 950 °C.

3.3. The austempered microstructure

The evolution of the austempered microstructure has been described in detail in a companion paper [3]. The low C austenite generated during austenitizing is transformed into bainitic ferrite and high C austenite during the stage I reaction. In the stage II reaction the high C austenite breaks down into ferrite and carbide. The development of the austempered structure can be traced by using the parameter $X_\gamma C_\gamma$ to follow the distribution of carbon between the phases involved in the stage I and stage II reactions. This procedure is adopted in this section because of the very strong relationship suggested by Shanmugam *et al.* [12] between fatigue strength and $X_\gamma C_\gamma$ shown in Fig. 4.

The C content of the low C austenite, C_γ^0, formed during austenitizing depends on the iron composition and the austenitizing temperature. This dependence has been expressed by the equation [13]

$$C_\gamma^0 = -0.435 + 0.335\times10^{-3}T_\gamma + 1.61\times10^{-6}T_\gamma^2 + 0.006(\text{Mn wt \%}) - 0.11(\text{Si wt \%}) - 0.07(\text{Ni wt \%}) + 0.014(\text{Cu wt \%}) - 0.30(\text{Mo wt \%}) \quad (1)$$

In the present iron C_γ^0 is 0.65, 0.74 and 0.95 wt % for austenitizing temperatures of 870, 900 and 950 °C, respectively. During austempering the carbon is redistributed between unreacted austenite, bainitic ferrite, high C austenite and carbide. A mass balance equation

$$C_\gamma^0 = X_\gamma C_\gamma + X_\gamma^0 C_\gamma^0 + X_\alpha C_\alpha + X_C C_C \quad (2)$$

where X_γ, X_γ^0, X_α and X_C are the amounts of high C austenite, low C austenite, bainitic ferrite and carbide, respectively, and where C_γ, C_γ^0, C_α and C_C are the C content of high C austenite, low C austenite, bainitic ferrite and carbide, respectively. As the value of C_α is small, the term $X_\alpha C_\alpha$ can be neglected, reducing Equation 2 to

$$C_\gamma^0 = X_\gamma C_\gamma + X_\gamma^0 C_\gamma^0 + X_C C_C \quad (3)$$

This equation can be used to follow the evolution of the austempered microstructure at 370 °C. After 30 min austempering following austenitizing at 870 °C, Fig. 5 shows that the $X_\gamma C_\gamma$ value is 0.60 wt %. The amount of unreacted, low C austenite is 3.5 wt % (X_γ^0 is 0.035 wt %) and, as the value of C_γ^0 is 0.65 wt %, the product $X_\gamma^0 C_\gamma^0$ is 0.02 wt %. These calculations suggest that unreacted, low C austenite (in the form of martensite), bainitic ferrite and high C austenite are present in the microstructure. The stage I reaction is near to completion. After 90 min austempering, the value of $X_\gamma C_\gamma$ is approaching C_γ^0 suggesting that the matrix structure is the ideal structure of bainitic ferrite

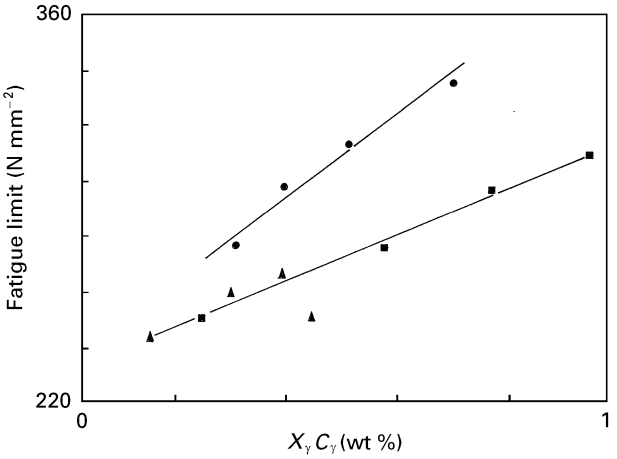

Figure 4 Variation of fatigue strength with the parameter $X_\gamma C_\gamma$ due to Shanmugam *et al.* [12]: (●) at 900 °C/400 °C, (■) at 1050 °C/280 °C, and (▲) 1050 °C/400 °C for austenitizing/austempering temperatures, respectively.

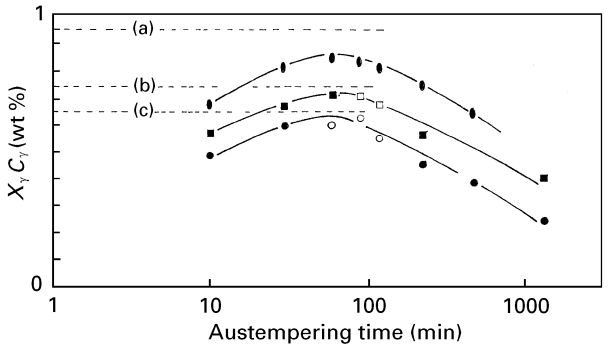

Figure 5 Variation of the parameter $X_\gamma C_\gamma$ with austempering time: (a) C_γ^0 at 950 °C, (b) C_γ^0 at 900 °C, and (c) C_γ^0 at 870 °C. Unfilled symbols represent conditions producing an ausferrite structure. Filled symbols represent conditions producing an austempered structure containing martensite and/or carbide. (○) 870/370, (□) 900/370, (□) 950/370 for austenitizing temperatures (°C), respectively.

and high C austenite, commonly called ausferrite. The X_γ^0 value has fallen to 0.02 wt % and the $X_\gamma^0 C_\gamma^0$ value is 0.013 wt %. After 120 min, the value of $X_\gamma C_\gamma$ has fallen to 0.55 wt %. The X_γ^0 value has fallen to 0.01 wt % leaving a value of 0.09 wt % for $X_C C_C$ from Equation 3. This suggests that the matrix structure consists of high C austenite ferrite, a little unreacted austenite and some carbide. Hence the stage I reaction is considered completed [unreacted austenite volume (UAV) fraction = 1%] and the stage II reaction has started. After 240 min the $X_\gamma C_\gamma$ value has fallen to 0.44 wt %. The difference between C_γ^0 and $X_\gamma C_\gamma$ levels has increased to 0.21 wt % and is attributed to $X_C C_C$. Thus the stage II reaction is more advanced.

A similar pattern of behaviour is observed with an austenitizing temperature of 900 °C. The higher austenitizing temperature increases the C_γ^0 value to 0.74 wt % and reduces the driving force for the stage I reaction. After 30 min austempering the $X_\gamma C_\gamma$ value is 0.68 wt % and the X_γ^0 value is 0.08 wt %. Hence, as for an austenitizing temperature of 870 °C, the matrix structure consists of martensite, bainitic ferrite and high C austenite but with a higher level of martensite. After 90 min the $X_\gamma C_\gamma$ level has increased to 0.72 wt % and the X_γ^0 value is 0.04 wt %. Hence the structure is the same as for 30 min but the amount of martensite has reduced as the stage I reaction proceeds. After 240 min the $X_\gamma C_\gamma$ value has fallen to 0.56 wt % with X_γ^0 reduced to 0.015 wt %. Hence the $X_C C_C$ value is 0.18 wt % indicating that the stage II reaction has occurred to approximately the same extent as for 240 min austempering after austenitizing at 870 °C.

The behaviour at an austenitizing temperature of 950 °C follows a similar pattern but at corresponding times the value of X_γ^0 is higher. Its value is 0.15, 0.09 0.07 and 0.06 wt % at 30, 90, 120 and 240 min. Consequently martensite is present in the matrix at all these austempering times. At 240 min $X_\gamma C_\gamma$ is 0.75 wt % and $X_\gamma^0 C_\gamma^0$ is 0.06 wt %. Hence from Equation 3 $X_C C_C$ is 0.14 wt %. Consequently, after 240 min the stage I reaction is incomplete and the stage II reaction has started.

The presence of martensite and carbide in the austempered microstructure has been shown to be detrimental to tensile properties in the companion paper. The filled symbols in Fig. 5 represent austempered matrix structures that failed to satisfy the ASTM standard. The open symbols represent structures that satisfied the standard.

3.4. The relationship between fatigue properties and austempered microstructure

Previous studies [14, 15] have shown that fatigue cracks initiate at the interface between graphite nodules and the matrix or at pores. The fatigue crack then follows the path of least resistance through the matrix between nodules. Fig. 6 shows crack initiation at the nodule matrix interface and a crack path through the path of least resistance at the intercellular boundary after nucleation at a pore. The variation of fatigue strength with $X_\gamma C_\gamma$ measured for different austempered matrix structures in this study is shown in Fig. 7. Comparison with Fig. 4 shows that the present study does not show the same well defined relationship between fatigue strength and $X_\gamma C_\gamma$. The majority of the measurements in Fig. 4 were made for a very high austenitizing temperature of 1050 °C and revealed a pattern of austempering behaviour that has not been reported previously at lower austenitizing temperatures. For example, it has been shown in several previous studies that for a constant austenitizing

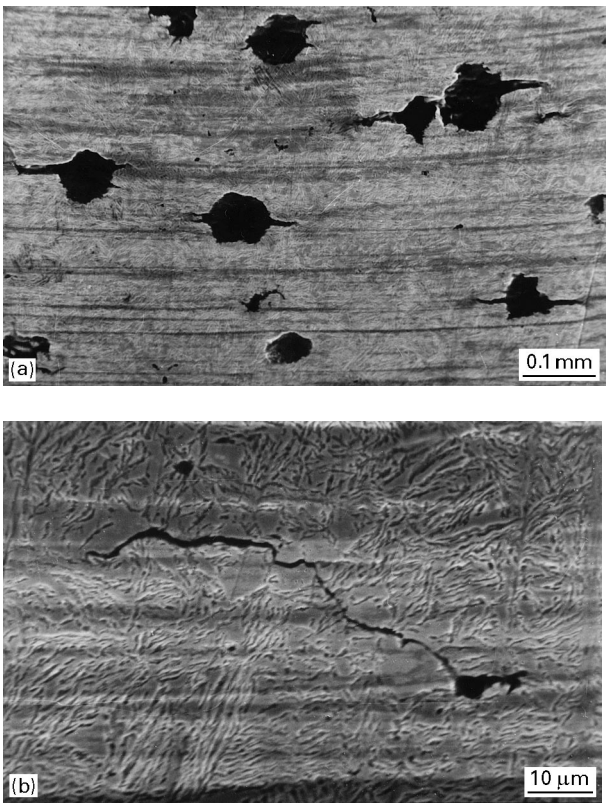

Figure 6 Microstructures showing (a) cracks initiating at the graphite–matrix interface in a partially fatigued specimen and (b) a crack propagating from a pore through an intercellular boundary containing martensite.

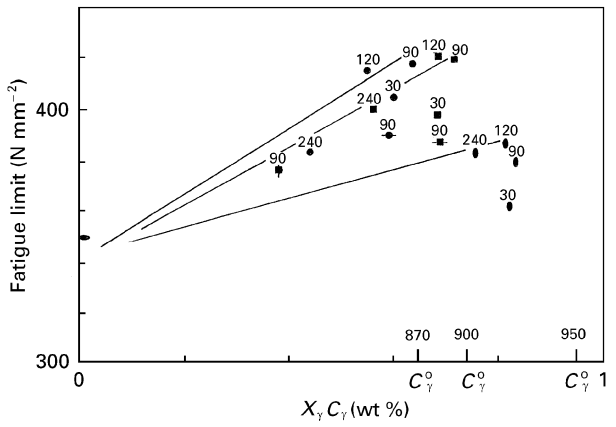

Figure 7 Variation of fatigue strength with the parameter $X_{\gamma}C_{\gamma}$ for various austempered conditions: (⬭) as-cast, (●) 870/370, (–●–) 870/400, (■) 900/315, (■) 900/370, (–■–) 900/400, and (⬮) 950/370 austenitizing/austempering temperatures (°C) respectively.

temperature the value of $X_{\gamma}C_{\gamma}$ is much higher at higher austempering temperatures such as 400 °C than at lower austempering temperatures such as 280 °C. This is due to the formation of carbide in the bainitic ferrite phase during the state I reaction at lower austempering temperatures. The measurements in Fig. 4 suggest that the $X_{\gamma}C_{\gamma}$ value is much greater for an austempering temperature of 280 °C for an austenitizing temperature of 1050 °C.

Despite the differences observed in austempering behaviours there is evidence of similar trends in the dependence of fatigue strength on austempered microstructure in the two studies. The resistance to crack propagation and the fatigue strength would be expected to depend on the amount and nature of the high C austenite and the fineness of the austempered structure. A common feature of both studies is that the highest fatigue strength is observed in austempered structures characterized by $X_{\gamma}C_{\gamma}$ approaching C^{0}_{γ}, that is, with an ausferrite structure at the higher austempering temperatures used in the present study. It can be seen that at each of the austenitizing temperatures as the austempering time at 370 °C increases from 30 to 120 min the fatigue strength increases. This corresponds to a reduction in the amount of unreacted, low C austenite in the austempered structure. This low C austenite is thermally unstable and transforms to martensite that above a 3 wt % level forms continuous paths in the intercellular boundaries of the austempered structure reducing the resistance to crack growth and the fatigue strength. This behaviour is illustrated in Fig. 6. At constant austempering time the effect is greater the higher the austenitizing temperature. After 240 min austempering, the stage II reaction has started for all austenitizing temperatures with carbide precipitation at ferrite–austenite phase boundaries causing a reduction in the fatigue strength.

In an ausferrite structure at constant austenitizing and austempering temperatures the fatigue strength might be expected to increase with X_{γ} and C_{γ} due to the excellent strain hardening behaviour of austenite and the strain ageing behaviour associated with carbon. There is some evidence for this in Fig. 7. Evidence of mechanical instability of the high C austenite in the form of martensite formation ahead of the fatigue crack was not found in the present study in agreement with the findings of Boschen *et al.* [16].

Finally, the fatigue strength should be increased with a finer and more uniformly distributed microstructure. This can be achieved by reducing the austenitizing and austempering temperatures. The effect of austenitizing temperature is very evident in Fig. 4. The same effect is present in Fig. 7 in which three linear relationships are drawn to indicate the dependence of fatigue strength of an ausferrite structure on $X_{\gamma}C_{\gamma}$ for austenitizing temperatures of 870, 900 and 950 °C. The higher fatigue strength is associated with the lower austenitizing temperature. The measurements recorded for 90 min austempering for austenitizing temperatures of 870 and 900 °C show that for both austenitizing temperatures reducing the austempering temperature from 400 to 370 °C increases the fatigue strength.

It is hoped to comment further on the relationship between fatigue strength and austempered temperature microstructure when measurements at higher austenitizing temperatures and lower austempering temperatures have been completed.

4. Conclusions

Measurements of the rotating bending fatigue strength of irons austempered at 370 and 400 °C after austenitizing at 870, 900 and 950 °C are presented and related to the microstructure of the austempered iron. The well defined relationship between fatigue strength and the parameter $X_{\gamma}C_{\gamma}$ observed in a previous study is not confirmed although several similar trends in behaviour are identified. The present results, which concentrate on higher austempering temperatures, show:

1. For an austenitizing temperature of 900 °C, the fatigue strength increases with increasing austempering temperature in the range 300–370 °C and then decreases; whereas the UTS decreases continuously over the austempering temperature range 300–400 °C.

2. The highest fatigue strength is observed in an ausferrite structure with a high $X_{\gamma}C_{\gamma}$ value; the presence of thermally unstable, unreacted austenite (in the form of martensite) at short austempering times and carbide at long austempering times reduces the fatigue strength.

3. A finer ausferrite structure achieved at lower austenitizing and austempering temperatures increases the fatigue strength.

Acknowledgements

M. B. would like to thank the Iranian Government for providing financial support. The authors would like to thank Professor G. W. Lorimer for providing research facilities.

References

1. B. V. KOVACS, *J. Heat Treatment* **5** (1987) 55.
2. M. BAHMANI, R. ELLIOTT and N. VARAHRAM, *Int. Cast Met. Res. J.* submitted.
3. M. BAHMANI, N. VARAHRAM and R. ELLIOTT, *J. Mater. Sci.* submitted.
4. L. ROBINSON, W. SPEAR and S. SESHAN, *AFS Trans.* **97** (1989) 345.
5. K. JOKIPII, in Proceedings of the First International Conference on austempered ductile iron (American Society for Metals, Metals Park, OH, 1984) p. 135.
6. K. HORNUNG and W. HAUKE, in *ibid.* p. 185.
7. R. A. HARDING, *Met. Mater.* **2** (1986) 65.
8. M. GRECH and J. M. YOUNG, *AFS Trans.* **98** (1990) 341.
9. G. P. FAUBERT, D. J. MOORE and K. B. RUNDMAN, *ibid.* **99** (1991) 759.
10. *Idem*, *ibid.* **100** (1992) 563.
11. K. L. HAYRYNEN, D. J. MOORE and K. B. RUNDMAN, *ibid.* **101** (1993) 93.
12. P. SHANMUGAM, P. PRASAD RAO, K. RAJENDRA UDUPA and N. VENKATARAMAN, *J. Mater. Sci.* **29** (1994) 4933.
13. F. NEUMANN, in "Recent research in cast iron", edited by H. D. Merchant (Gordon & Beach, 1965) p. 659.
14. R. VOIGT, H. DHANE and L. ELDOKY, in Proceedings of the First International Conference on austempered ductile iron (American Society for Metals, Metals Park, OH, 1984) p. 327.
15. K. P. JEN, J. WU and S. KIM, *AFS Trans.* **101** (1993) 833.
16. R. BOSCHEN, H. BOMAS, P. MAYR and H. VETTERS, in Proceedings of the 1991 World Conference on austempered ductile iron, Chicago, 1991, p. 468.

Received 7 August 1996
and accepted 26 February 1997